JACS
JOURNAL OF THE AMERICAN CHEMICAL SOCIETY
Communication
pubs.acs.org/JACS

Design of Pt–Pd Binary Superlattices Exploiting Shape Effects and Synergistic Effects for Oxygen Reduction Reactions

Yijin Kang,[‡,†] Xingchen Ye,[‡,†] Jun Chen,[§] Yun Cai,[∥] Rosa E. Diaz,[⊥] Radoslav R. Adzic,[∥] Eric A. Stach,[⊥] and Christopher B. Murray*[,‡,§]

Departments of [‡]Chemistry and [§]Materials Science and Engineering, University of Pennsylvania, Philadelphia, Pennsylvania 19104, United States

[∥]Department of Chemistry and [⊥]Center for Functional Nanomaterials, Brookhaven National Laboratory, Upton, New York 11973, United States

Supporting Information

ABSTRACT: Large-area icosahedral-AB_{13}-type Pt–Pd binary superlattices (BNSLs) are fabricated through self-assembly of 6 nm Pd nanocrystals (NCs) and 13 nm Pt octahedra at a liquid–air interface. The Pt–Pd BNSLs enable a high activity toward electrocatalysis of oxygen reduction reaction (ORR) by successfully exploiting the shape effects of Pt NCs and synergistic effects of Pt–Pd into a single crystalline nanostructure. The Pt–Pd BNSLs are promising catalysts for the oxygen electrode of fuel cells.

The well-controlled synthesis of colloidal nanocrystals (NCs) makes the use of nanomaterials possible in a number of applications, including electronics,[1−3] magnetics,[4,5] optics,[1,6,7] and catalysis.[8−17] Bottom-up fabrication of nanostructures from colloidal nanocrystals such as self-assembly provides new possibilities in preparing functional materials.[18−21] Nanocrystal superlattices have been prepared through self-assembly as early as in 1995,[22] and the fabrication of multicomponent superlattices has received great attention due to the possibility of combining the chemical and physical properties of different materials within a single nanostructure to exploit the unique physical phenomena and materials.[2−5,19,23−27] The interaction between different materials in the multicomponent superlattice (e.g., binary superlattices) has been shown to be interesting in electronics[3,28] and magnetics.[5,25] However, the application of multicomponent nanocrystal superlattices in catalysis has not yet been reported.

Previous research has indicated that Pd can promote the performance of Pt catalysts for various catalytic reactions.[29−34] Particularly in the oxygen reduction reaction (ORR), Pd and Pt show a "synergistic effect" that Pd–Pt electrocatalysts exhibit superior activity than individual Pt or Pd electrocatalyst.[29,30,33−37] This synergistic effect is attributed to the interaction of Pt–Pd, modifying the Pt d-band center, weakening the electronic interaction between surface Pt atoms and oxygenated species (e.g., OH_{ads}), thereby enhancing ORR activity. It is well-known that Pt(111) possesses higher ORR activity than Pt(100).[38] Therefore, Pd-promoted Pt catalysts with Pt(111) facets are highly desirable. Unfortunately, it is challenging to prepare a catalyst with this specific structure. The binary superlattice (BNSL) offers a new route for the catalyst design: physically attaching Pd onto Pt(111). We extend this principle further, and design a 3-dimensional (3D) BNSL beyond spherical building blocks, exploiting Pt octahedra together with Pd spheres to enhance the performance of these materials for electrocatalysis of ORR.

We self-assemble 6 nm (diameter) near-spherical Pd NCs (Figure S1) and 13 nm (vertex-to-vertex distance) Pt octahedra (Figure S2) which expose (111) facets, into a Pt–Pd BNSL. In Figures 1a and S3–S5, transmission electron microscopy (TEM) image shows that Pd NCs and Pt octahedra take positions in a highly ordered superlattice to form a thin film of Pt–Pd BNSL with uniform thickness. The high angle annular dark field scanning transmission electron microscopy (HAADF-STEM) image in Figure 1b clearly shows the octahedral shape. Scanning electron microscopy (SEM) images (Figures 1c and S6) exhibits a flat terrace of the Pt–Pd BNSL, reminiscent of the single crystal surfaces which are frequently used as models to study electrocatalysis, but now modulated at the nanoscale. Energy-dispersive X-ray spectroscopy (EDX) mapping using STEM (Figure 1d–f) confirms the composition of the Pt–Pd BNSL. The images shown in Figure 1 are the [001] projection of an icosahedral-AB_{13} (ico-AB_{13}) structure. The proposed structural model is shown in the inset of Figure 1c. The unit cell of the ico-AB_{13} structure consists of 8 Pt icosahedra and 104 Pd spheres. Each Pt octahedron is in contact with 12 Pd spheres. The AB_{13}-type Pt–Pd BNSL is phase-pure; no other BNSL structure is observed in thin films of AB_{13}-type Pt–Pd BNSLs.

TEM and HAADF-STEM images are two-dimensional (2D) projection of 3D structures, and SEM images are limited, in that they present surface sensitive information. Therefore, these conventional electron microscopy images are not sufficient to ascertain the structure of BNSLs. To uniquely assign the structure, we employ a crystallographic analysis procedure using a dual-axis tomography TEM holder.[39] As shown in Figure 2, we start from the [001]-oriented domain, and via [015], [013], and [012], tilt to the [011] zone axis. This tilt series demonstrates that the BNSL has an ico-AB_{13} structure (shown in inset of Figure 1c) analogous to the $NaZn_{13}$ intermetallic, this is, similar to that of many reported AB_{13}-type BNSLs built with spherical building blocks.[19,25,39]

Received: October 2, 2012
Published: December 7, 2012

   dx.doi.org/10.1021/ja3097527 | J. Am. Chem. Soc. 2013, 135, 42–45

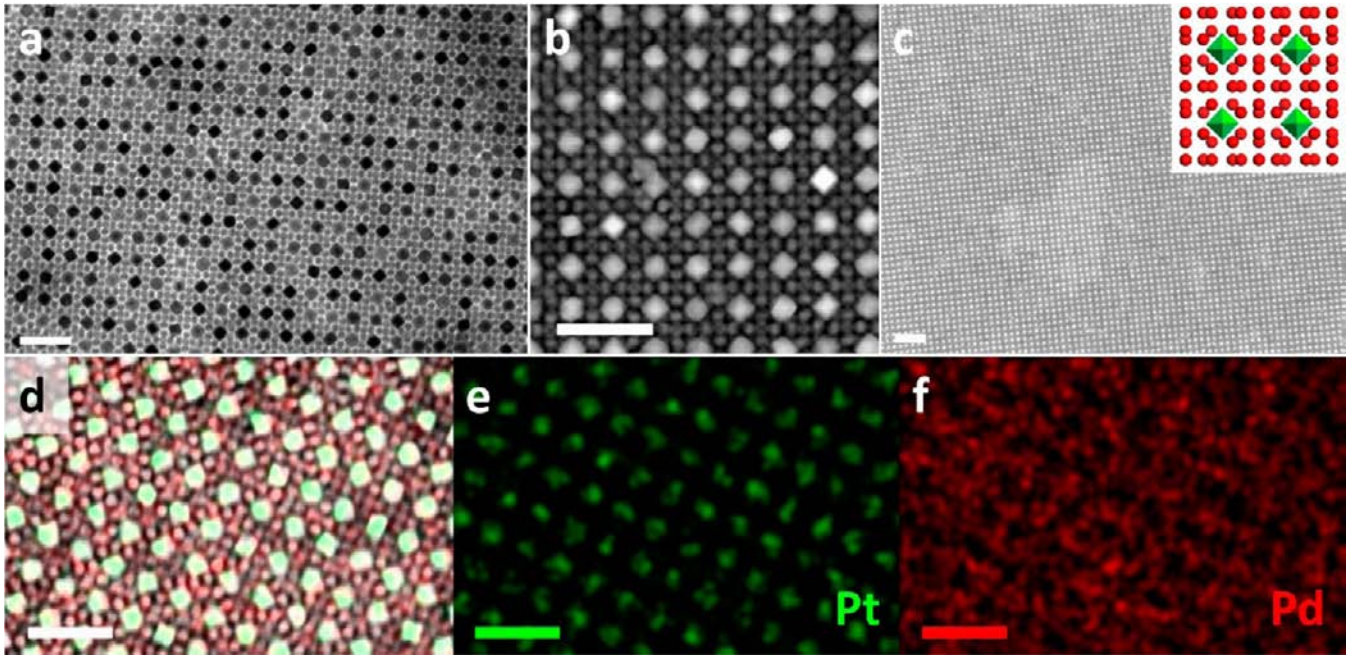

Figure 1. (a) TEM, (b) STEM-HAADF, and (c) SEM images of Pt−Pd AB_{13}-type BNSL. (d−f) STEM-EDX-mapping (green, Pt; red, Pd, f shows overlaps of STEM image and EDX-mappings) of Pt−Pd BNSLs. Inset of c, proposed structural model: a unit cell of ico-AB_{13} BNSL (A, Pt octahedron in green; B, Pd sphere in red). Scale bars: (a, b, d−f) 50 nm, (c) 100 nm.

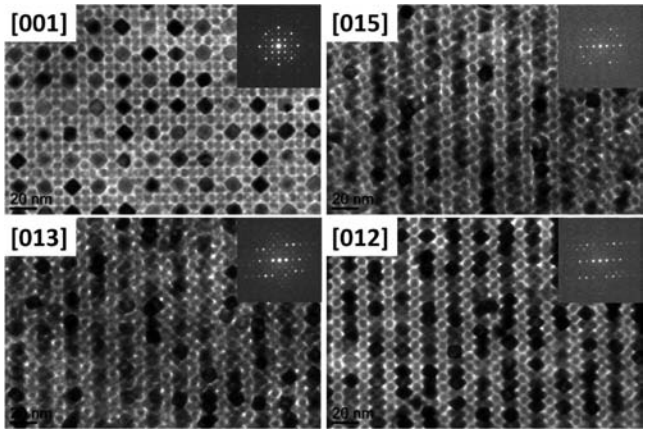

Figure 2. Crystallographic analysis of Pt−Pd BNSLs confirms the ico-AB_{13}-type structure analogous to $NaZn_{13}$. Tilting sequence: [001] → [015] → [013] → [012] zone axes.

To test the electrochemical properties of the Pt−Pd BNSL, the film of Pt−Pd BNSL is assembled at the liquid−air interface and transferred onto a 6 mm glassy carbon disc.[25] A UV/ozone treatment (10 h) is used to remove the organic capping agents, and a thermal treatment (180 °C, 30 min) produces direct contacts among nanocrystals for an effective Pt−Pd interaction. Before the electrochemical measurements, CO-striping is utilized to further clean the surface of the BNSL catalyst.[36] Single component Pd nanocrystal superlattices (Figure S1) and superlattices of Pt octahedra (Figure S2), as well as thin films of randomly mixed Pt octahedra and Pd nanocrystals (Figures S8, S9) are prepared and treated by the same procedure. All the thin films deposited at the liquid−air interface have similar thickness, and thus, they have similar loading of catalysts over the same area of electrodes.

The cyclic voltammograms (CVs) of Pd nanocrystals, Pt octahedra, randomly mixed Pt and Pd nanocrystals, and Pt−Pd BNSL are presented in Figure 3a. In the region of H-adsorption and H-desorption (i.e., 0.05−0.4 V), CV of Pd nanocrystals shows two peaks at 0.10 and 0.21 V. CV of Pt octahedra has a characteristic peak corresponding to Pt(111). The random mixture has a single sharp peak at 0.19 V, which is similar to that reported in the CV curve on an epitaxial Pd film on Pt(111).[40] CV of the Pt−Pd BNSL exhibits a broad peak around 0.2 V. All three Pt-containing thin films have similar peak areas (i.e., a similar amount of adsorbed H atoms), confirming that the loading of catalysts on each sample is comparable. This makes the following ORR measurements of nanocrystal thin films and Pt−Pd BNSL comparable.

ORR activities of nanocrystal films are tested on a rotating disc electrode (RDE) at a rotating speed of 1600 rpm, and the results are shown in Figure 3b. As Pd has a poor ORR activity compared to Pt, the mixture of Pt and Pd nanocrystals is expected to have an activity between that of Pd and Pt, if there is no synergistic effect. This result is observed on the random mixture of Pt and Pd nanocrystals, in which Pd and Pt NCs are significantly phase-segregated. In contrast, the ORR activity obtained with Pt−Pd BNSLs is better than that of the separate Pt and Pd samples. The kinetic current densities extracted from ORR polarization curves are shown in Figure 3c and Pt-loading normalized kinetic current densities are shown in Figure 3d. At 0.8 and 0.85 V, the kinetic current density obtained on Pt−Pd BNSL is approximately 2 and 4 times as high as that on the Pt octahedra and the random mixture, respectively. By normalizing the kinetic current densities with the mass of Pt, the Pt−Pd BNSL has an even higher activity than pure Pt octahedra, by a factor of 4 at 0.9 and 0.85 V (5 at 0.8 V), while the Pt−Pd random mixture shows a slightly higher activity than Pt octahedra. Incorporating Pd nanocrystals into an assembly of Pt octahedra exploits the high ORR activity on Pt(111) and captures the Pt−Pd synergistic effect together in a single nanostructured material, yielding enhancements that cannot be achieved by simply mixing the components.

dx.doi.org/10.1021/ja3097527 | J. Am. Chem. Soc. 2013, 135, 42−45

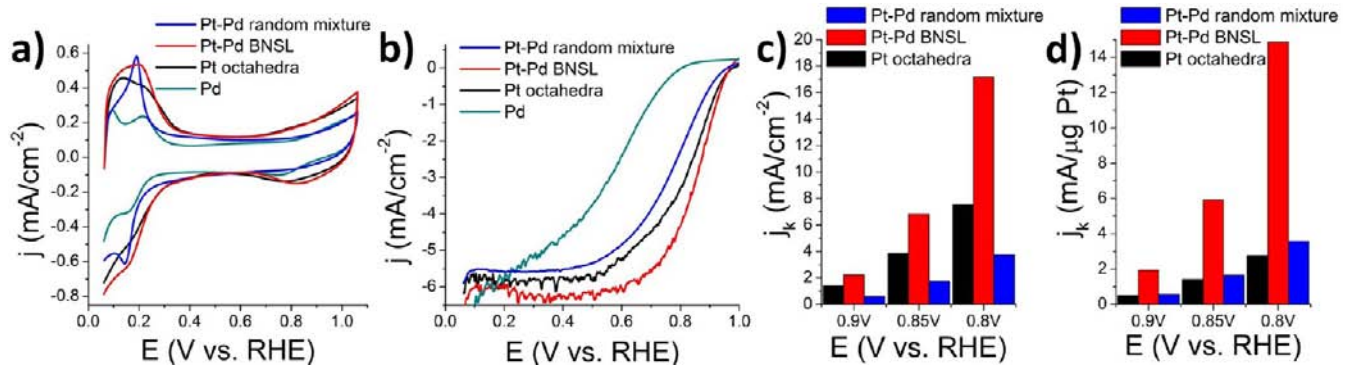

Figure 3. (a) CV curves and (b) ORR polarization curves of a Pt−Pd BNSL, random mixture of Pt−Pd NCs, Pd NCs and Pt octahedra. (c and d) Bar chart of kinetic current of Pt−Pd BNSL, random mixture of Pt−Pd NCs, and Pt octahedra at 0.9, 0.85, and 0.8 V.

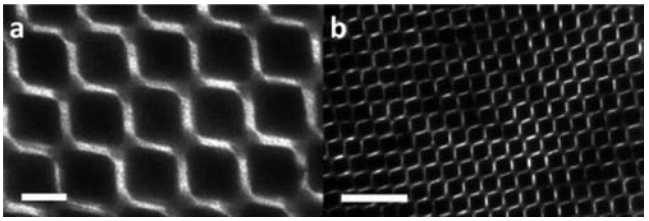

Figure 4. TEM images of AB-type Pt−Pd BNSL. Scale bars: (a) 10 nm, (b) 50 nm.

The Pt−Pd BNSLs in AB-type structure are also prepared (Figures 4 and S10). However, the phase-purity and the coverage have not been optimized to an extent that allows reliable property measurements.

In summary, we demonstrate a new method of catalyst design, which combines the shape effects and synergistic effects to produce a BNSL catalyst of Pt−Pd. Multicomponent NC superlattices represent model systems for the study of heterogeneous catalysis (including electrocatalysis), especially for the exploration of synergistic interactions between different metals as well as between metal and oxide supports.

■ ASSOCIATED CONTENT

Ⓢ Supporting Information

Details of experiments, additional TEM, SEM, and HAADF-STEM images. This material is available free of charge via the Internet at http://pubs.acs.org.

■ AUTHOR INFORMATION

Corresponding Author

cbmurray@sas.upenn.edu

Author Contributions

†These authors contributed equally.

Notes

The authors declare no competing financial interest.

■ ACKNOWLEDGMENTS

C.B.M. and Y.K. acknowledge the partial support from the National Science Foundation MRSEC DMR11-20901. X.Y. acknowledges the support from the Office of Naval Research (ONR) Multidisciplinary University Research Initiative (MURI) on Optical Metamaterials through award N00014-10-1-0942. J.C. acknowledges the DOE Office of ARPA-E for support under Award DE-AR0000123. Y.K.'s development of catalytic NCs was partially supported by the Nano/Bio Interface Center through the National Science Foundation NSEC DMR11-20901. C.B.M. thanks the Richard Perry University Professorship for the support of his supervisor role. Research carried out in part at the Center for Functional Nanomaterials (CFN) and Department of Chemistry, Brookhaven National Laboratory (BNL), which is supported by the U.S. Department of Energy, Office of Basic Energy Sciences, under Contract No. DE-AC02-98CH10886. We thank Charles Black and Fernando Camino for the support at CFN, Naoki Kikuchi from JEOL for the SEM images and David Vann at Department of Earth and Environmental Science (University of Pennsylvania) for assistance in ICP-OES.

■ REFERENCES

(1) Murray, C. B.; Norris, D. J.; Bawendi, M. G. *J. Am. Chem. Soc.* **1993**, *115*, 8706−8715.
(2) Redl, F. X.; Cho, K. S.; Murray, C. B.; O'Brien, S. *Nature* **2003**, *423*, 968−971.
(3) Talapin, D. V.; Murray, C. B. *Science* **2005**, *310*, 86−89.
(4) Sun, S. H.; Murray, C. B.; Weller, D.; Folks, L.; Moser, A. *Science* **2000**, *287*, 1989−1992.
(5) Chen, J.; Dong, A. G.; Cai, J.; Ye, X. C.; Kang, Y. J.; Kikkawa, J. M.; Murray, C. B. *Nano Lett.* **2010**, *10*, 5103−5108.
(6) Tao, A.; Sinsermsuksakul, P.; Yang, P. *Nat.e Nanotechnol.* **2007**, *2*, 435−440.
(7) Ye, X. C.; Collins, J. E.; Kang, Y. J.; Chen, J.; Chen, D. T. N.; Yodh, A. G.; Murray, C. B. *Proc. Natl. Acad. Sci. U.S.A.* **2010**, *107*, 22430−22435.
(8) Kang, Y. J.; Murray, C. B. *J. Am. Chem. Soc.* **2010**, *132*, 7568−7569.
(9) Kang, Y. J.; Ye, X. C.; Murray, C. B. *Angew. Chem., Int. Ed.* **2010**, *49*, 6156−6159.
(10) Wang, D. Y.; Kang, Y. J.; Doan-Nguyen, V.; Chen, J.; Kungas, R.; Wieder, N. L.; Bakhmutsky, K.; Gorte, R. J.; Murray, C. B. *Angew. Chem., Int. Ed.* **2011**, *50*, 4378−4381.
(11) Kang, Y. J.; Qi, L.; Li, M.; Diaz, R. E.; Su, D.; Adzic, R. R.; Stach, E.; Li, J.; Murray, C. B. *ACS Nano* **2012**, *6*, 2818−2825.
(12) Lee, I.; Delbecq, F.; Morales, R.; Albiter, M. A.; Zaera, F. *Nat. Mater.* **2009**, *8*, 132−138.
(13) Yamada, Y.; Tsung, C. K.; Huang, W.; Huo, Z. Y.; Habas, S. E.; Soejima, T.; Aliaga, C. E.; Somorjai, G. A.; Yang, P. D. *Nat. Chem.* **2011**, *3*, 372−376.
(14) Wang, C.; Daimon, H.; Lee, Y.; Kim, J.; Sun, S. *J. Am. Chem. Soc.* **2007**, *129*, 6974−6975.
(15) Wang, C.; Chi, M.; Li, D.; Strmcnik, D.; van der Vliett, D.; Wang, G.; Komanicky, V.; Chang, K.-C.; Paulikas, A. P.; Tripkovic, D.; Pearson, J.; More, K. L.; Markovic, N. M.; Stamenkovic, V. R. *J. Am. Chem. Soc.* **2011**, *133*, 14396−14403.
(16) Kang, Y. J.; Pyo, J. B.; Ye, X. C.; Gordon, T. R.; Murray, C. B. *ACS Nano* **2012**, *6*, 5642−5647.
(17) Zhang, J.; Yang, H.; Fang, J.; Zou, S. *Nano Lett.* **2010**, *10*, 638−644.

(18) Buck, M. R.; Bondi, J. F.; Schaak, R. E. *Nat. Chem.* **2012**, *4*, 37−44.
(19) Shevchenko, E. V.; Talapin, D. V.; Kotov, N. A.; O'Brien, S.; Murray, C. B. *Nature* **2006**, *439*, 55−59.
(20) Tang, Z. Y.; Zhang, Z. L.; Wang, Y.; Glotzer, S. C.; Kotov, N. A. *Science* **2006**, *314*, 274−278.
(21) Wang, C.; van der Vliet, D.; More, K. L.; Zaluzec, N. J.; Peng, S.; Sun, S. H.; Daimon, H.; Wang, G. F.; Greeley, J.; Pearson, J.; Paulikas, A. P.; Karapetrov, G.; Strmcnik, D.; Markovic, N. M.; Stamenkovic, V. R. *Nano Lett.* **2011**, *11*, 919−926.
(22) Murray, C. B.; Kagan, C. R.; Bawendi, M. G. *Science* **1995**, *270*, 1335−1338.
(23) Dumestre, F.; Chaudret, B.; Amiens, C.; Renaud, P.; Fejes, P. *Science* **2004**, *303*, 821−823.
(24) Smith, D. K.; Goodfellow, B.; Smilgies, D. M.; Korgel, B. A. *J. Am. Chem. Soc.* **2009**, *131*, 3281−3290.
(25) Dong, A. G.; Chen, J.; Vora, P. M.; Kikkawa, J. M.; Murray, C. B. *Nature* **2010**, *466*, 474−477.
(26) Henzie, J.; Gruenwald, M.; Widmer-Cooper, A.; Geissler, P. L.; Yang, P. *Nat. Mater.* **2012**, *11*, 131−137.
(27) Friedrich, H.; Gommes, C. J.; Overgaag, K.; Meeldijk, J. D.; Evers, W. H.; de Nijs, B.; Boneschanscher, M. P.; de Jongh, P. E.; Verkleij, A. J.; de Jong, K. P.; van Blaaderen, A.; Vanmaekelbergh, D. *Nano Lett.* **2009**, *9*, 2719−2724.
(28) Talapin, D. V.; Lee, J. S.; Kovalenko, M. V.; Shevchenko, E. V. *Chem. Rev.* **2010**, *110*, 389−458.
(29) Zhang, J. L.; Vukmirovic, M. B.; Sasaki, K.; Nilekar, A. U.; Mavrikakis, M.; Adzic, R. R. *J. Am. Chem. Soc.* **2005**, *127*, 12480−12481.
(30) Lim, B.; Jiang, M. J.; Camargo, P. H. C.; Cho, E. C.; Tao, J.; Lu, X. M.; Zhu, Y. M.; Xia, Y. N. *Science* **2009**, *324*, 1302−1305.
(31) Lee, H. J.; Habas, S. E.; Somorjai, G. A.; Yang, P. D. *J. Am. Chem. Soc.* **2008**, *130*, 5406−5407.
(32) Habas, S. E.; Lee, H.; Radmilovic, V.; Somorjai, G. A.; Yang, P. *Nat. Mater.* **2007**, *6*, 692−697.
(33) Wang, J. X.; Inada, H.; Wu, L. J.; Zhu, Y. M.; Choi, Y. M.; Liu, P.; Zhou, W. P.; Adzic, R. R. *J. Am. Chem. Soc.* **2009**, *131*, 17298−17302.
(34) Sasaki, K.; Naohara, H.; Cai, Y.; Choi, Y. M.; Liu, P.; Vukmirovic, M. B.; Wang, J. X.; Adzic, R. R. *Angew. Chem., Int. Ed.* **2010**, *49*, 8602−8607.
(35) Zhang, J. L.; Vukmirovic, M. B.; Xu, Y.; Mavrikakis, M.; Adzic, R. R. *Angew. Chem., Int. Ed.* **2005**, *44*, 2132−2135.
(36) Gong, K. P.; Vukmirovic, M. B.; Ma, C.; Zhu, Y. M.; Adzic, R. R. *J. Electroanal. Chem.* **2011**, *662*, 213−218.
(37) Peng, Z. M.; Yang, H. *J. Am. Chem. Soc.* **2009**, *131*, 7542−7543.
(38) Markovic, N. M.; Adzic, R. R.; Cahan, B. D.; Yeager, E. B. *J. Electroanal. Chem.* **1994**, *377*, 249−259.
(39) Chen, J.; Ye, X. C.; Murray, C. B. *ACS Nano* **2010**, *4*, 2374−2381.
(40) Markovic, N. M.; Lucas, C. A.; Climent, V.; Stamenkovic, V.; Ross, P. N. *Surf. Sci.* **2000**, *465*, 103−114.

dx.doi.org/10.1021/ja3097527 | *J. Am. Chem. Soc.* 2013, 135, 42−45